

2006

Performance and Spectral Analysis of Q2PSK and CE Q2PSK Systems in Ideal Bandlimited Channels

Milton I. Quinteros
University of New Orleans

Edit J. Kaminsky
University of New Orleans, ejbourge@uno.edu

Kenneth V. Cartwright
College of The Bahamas

Follow this and additional works at: https://scholarworks.uno.edu/ee_facpubs



Part of the [Electrical and Electronics Commons](#)

Recommended Citation

Quinteros, M., E. Kaminsky and K. Cartwright, "Performance and Spectral Analysis of Q2PSK and CE Q2PSK Systems in Ideal Bandlimited Channels", IEEE Globecom 2014, 8-12 Dec. 2014, 3621-3626.

This Conference Proceeding is brought to you for free and open access by the Department of Electrical Engineering at ScholarWorks@UNO. It has been accepted for inclusion in Electrical Engineering Faculty Publications by an authorized administrator of ScholarWorks@UNO. For more information, please contact scholarworks@uno.edu.

Performance and Spectral Analysis of Q²PSK and CEQ²PSK Systems in Ideal Bandlimited Channels

Milton I. Quinteros

Dept. of Electrical Engineering
EN 616A Lakefront Campus
University of New Orleans
New Orleans, LA 70148, U.S.A.
Email: mquinter@uno.edu

Edit J. Kaminsky

Dept. of Electrical Engineering
EN 846 Lakefront Campus
University of New Orleans
New Orleans, LA 70148, U.S.A.
Email: ejbourge@uno.edu

Kenneth V. Cartwright

School of Mathematics, Physics and Technology
College of The Bahamas
P.O. Box N4912
Nassau, Bahamas
Email: kvc@batelnet.bs

Abstract—The authors present theoretical performance analysis and simulation results for Quadrature-Quadrature Phase Shift Keying (Q²PSK), Constant Envelope (CE) Q²PSK, and trellis-coded 16D CEQ²PSK in ideal bandlimited channels of various bandwidths. The performance of receivers with and without channel estimation is reported. Spectral analysis is presented for each system, in addition to MSK and expanded uncoded 16D CEQ²PSK. We show that the effects of bandlimiting are most severe for Q²PSK. Knowledge of the channel information aids 4D CEQ²PSK the least. Only 6.8 dB of SNR is needed for the TCM system for a bit error rate of 10⁻⁵ for the narrowest channel bandwidth studied here, if the receiver has knowledge of the channel.

Index Terms—Q²PSK, CEQ²PSK, bandlimited channel, spectral efficiency, multidimensional TCM, constant envelope.

I. INTRODUCTION

The search for appropriate classes of signals and methods to mitigate medium disturbances has driven much of communications research. Researchers have investigated the performance of different sets of signals on a variety of channels which are limited in transmission power and available spectrum. In classical uncoded modulation systems, an increase in transmission efficiency might be accomplished by increasing the dimensionality of the signal space (see [1] and references therein).

Over the last few decades, authors have shown interest in a four-dimensional (4D) modulation scheme proposed by Saha and Birdsall in [2]: Quadrature-Quadrature Phase Shift Keying (Q²PSK). Because Q²PSK uses the space more efficiently than conventional QPSK and Minimum Shift Keying (MSK), Q²PSK provides increased spectral efficiency [3]–[6]. Indeed, Q²PSK and its variants have been considered by several authors because of the attractive possibility of spectral and power efficiency [4]–[16].

Q²PSK is reported to achieve 4 bits per modulation interval but lacks constant envelope which is a desired feature for nonlinear channels such as the satellite path [14]. If parity check coding is imposed at the input of the Q²PSK modulator, 4D Constant Envelope Quadrature-Quadrature Phase Shift keying (CEQ²PSK) is obtained [2,3,17] at the cost of a reduction in the information rate to 3 bits per modulation interval.

Westra et al. reported multilevel forms of Q²PSK in [7] to increase the effective data throughput. Saha and El-Ghandour introduced differential phase Q²PSK in [8], and Korn and Wei analyzed the performance on mobile satellite channels in [10]. Offset Q²PSK, which attains lower peak to average power ratio than Q²PSK, was presented in [15]. In [17], two 16D constellations that use four consecutive signalling intervals of CEQ²PSK were introduced: an unexpanded 16D CEQ²PSK constellation of 4096 signal points and an expanded 16D CEQ²PSK constellation of 8192 points. The unexpanded constellation has an information rate of 12 bits per 16D interval while the expanded constellation may be used to transmit 13 bits per 16D interval or to incorporate error correction coding [13].

Various implementations of Q²PSK combined with bandwidth efficient coding techniques such as Multidimensional Trellis Coded Modulation (MTCM) [18] have been presented [14,19,20]. In contrast to the conventional MTCM implementations, Quinteros et al. [13] used a technique proposed by Kaminsky in [21,22] to obtain a 16D TCM CEQ²PSK system that suffers no loss due to constellation expansion. Most recently, [16] used the same technique with a 32D CEQ²PSK constellation.

In this paper, we further analyze the performance of 4D Q²PSK in [3] and also present analysis for 4D CEQ²PSK and a trellis encoded 16D CEQ²PSK system in the bandlimited additive white Gaussian noise (AWGN) channel. In particular, we assume ideal filters of baseband bandwidth $\frac{0.6}{T}$ and $\frac{1}{T}$, where $2T$ is the 4D symbol interval (i.e., the bit interval, T_b is $T/2$) with perfect knowledge of the phase. In our simulations, we implement a receiver that assumes knowledge of the channel and one that doesn't (i.e., the receiver uses reference pulses which are not bandlimited). A discrete implementation of a finite-length maximum likelihood detector is employed in all cases; this is equivalent to the hardware detector in [11], optimum when no Inter-Symbol Interference (ISI) and no Cross-ISI (CISI) are present. In addition, we briefly present spectral analysis of all these systems.

We show that for very narrow channels the use of channel estimation aids the 16D TCM system more than the others and that knowledge of the channel is more important for Q²PSK

than for its 4D constant envelope counterpart at all bandwidths. Losses due to finite channel bandwidth are most severe for Q²PSK. At the narrowest bandwidth considered here, $0.6/T$, the gain of the 16D TCM system is 2 dB at a probability of bit error of 10^{-5} . Furthermore, we show that the performance of Saha's bit-by-bit suboptimum detector [3] may be considerably improved upon with little increase in complexity.

The rest of this paper is organized as follows: In Section II, brief descriptions of Q²PSK, CEQ²PSK, and 16D CEQ²PSK are presented. In Section III we describe the channel model, followed in Section IV by discussion of the receiver and the signals therein. Analysis of the probability of error in bandlimited channels with finite ISI and CISI is given in Section V, along with presentation of the spectral analysis. Results are given in Section VI. Conclusions and suggestions for further work are given in Section VII, followed by cited references.

II. BRIEF REVIEW OF Q²PSK

In this section, we briefly discuss the following constellations: 4D Q²PSK [2], Saha's 4D CEQ²PSK [3], Cartwright's 4D CEQ²PSK [17], and both unexpanded and expanded 16D CEQ²PSK [13].

A. 4D Q²PSK

The 4D Q²PSK modulation technique was introduced in [2] and uses the following transmitted signal:

$$S_q(t) = \sum_{i=1}^4 b_i(t)s_i(t), \quad (1)$$

where $b_i(t)$, $i = 1, \dots, 4$, is the value of the original bit i of duration $T/2$ prior to the serial to parallel conversion and of duration $2T$ after [2], and the passband modulating signal set $\{s_i(t)\}$, $i = 1, \dots, 4$, is:

$$s_1(t) = p_1(t) \cos(2\pi f_c t), \quad |t| \leq T \quad (2a)$$

$$s_2(t) = p_2(t) \cos(2\pi f_c t), \quad |t| \leq T \quad (2b)$$

$$s_3(t) = p_1(t) \sin(2\pi f_c t), \quad |t| \leq T \quad (2c)$$

$$s_4(t) = p_2(t) \sin(2\pi f_c t), \quad |t| \leq T, \quad (2d)$$

with orthogonal half-sinusoidal pulses $p_1(t) = \cos(\pi t/2T)$ and $p_2(t) = \sin(\pi t/2T)$, for $|t| \leq T$, and 0 otherwise. The carrier frequency, f_c , should be $\frac{n}{4T}$ with $n \geq 2$, and T is the duration of 2 bits. There are 16 symbols that form this non-constant envelope signal set with efficiency of 4 bits per modulation interval.

Using the baseband equivalent model for (1), the k^{th} transmitted Q²PSK signal is represented as:

$$S_k(t) = b_{1,k}p_1(t - 2kT) + b_{2,k}p_2(t - 2kT) + j[b_{3,k}p_1(t - 2kT) + b_{4,k}p_2(t - 2kT)]. \quad (3)$$

B. 4D CEQ²PSK

In [2] and [17], two constant envelope 4D constellations were introduced, each with an MSED of 8 for unit energy: Saha's CEQ²PSK and Cartwright's CEQ²PSK, respectively. Constant envelope is obtained by using a rate-3/4 block

encoder at the input of the Q²PSK modulator, where the fourth output bit is an odd parity check bit [2]. Three information input bits $\{b_1, b_2, b_3\}$ generate code words $\{b_1, b_2, b_3, b_4\}$ such that the eight possible transmitted signals for Saha's CEQ²PSK are $S_1 = [a, a, b, -b]$ and $S_2 = [a, -a, b, b]$. For Cartwright's CEQ²PSK, we have $S_{1r} = [0, \sqrt{2}a, \sqrt{2}b, 0]$ and $S_{2r} = [\sqrt{2}a, 0, 0, \sqrt{2}b]$. In both cases, a, b are either ± 1 . In order for the envelope to be constant, $b_1b_2 + b_3b_4 = 0$.

C. 16D CEQ²PSK

1) *Unexpanded 16D CEQ²PSK*: In [17], two 16D constellations were produced by concatenating either four consecutive CEQ²PSK symbols from Saha's constellation or four consecutive CEQ²PSK from Cartwright's constellation. Each of these 16D signal sets contains 4096 constant envelope points and has an MSED of 8 for unit energy.

2) *Expanded 16D CEQ²PSK*: The expanded 16D CEQ²PSK constellation is the union of the two 16D CEQ²PSK in subsection 1) above, and has 8192 points; the expanded constellation has twice as many points as either unexpanded 16D CEQ²PSK constellation but still maintains an MSED of 8. There are 16 points (i.e., an error coefficient of 2 when normalized to 2D) at the second smallest squared distance of 9.373 which slightly degrades the performance over the unexpanded constellation, particularly for low SNR [17]. In [13], this expanded constellation was used to allow 1 bit of redundancy per 16D to be introduced through a convolutional encoder in a TCM system. This 16D TCM CEQ²PSK system is also studied here. Improved probability of error performance is achieved while maintaining constant envelope with a slight increase in system complexity.

III. CHANNEL MODEL

Most transmission media alter the transmitted signals in some way, especially when the channel has limited bandwidth [23]. In this section, we define the simple ideal bandlimited additive white Gaussian noise (AWGN) channel we use in our analysis and simulations, and show the effects of bandlimiting on Q²PSK and CEQ²PSK.

Forney and Ungerboeck defined the ideal bandlimited channel with flat frequency response within baseband bandwidth B in [1]. The signal $s(t)$ passes through a dispersive channel with impulse response $h(t)$ and zero-mean AWGN $n(t)$. The received signal is:

$$r(t) = s(t) * h(t) + n(t), \quad (4)$$

with $h(t)$ given by:

$$h(t) = \frac{\sin(2\pi Bt)}{\pi t}. \quad (5)$$

We consider two channel bandwidths, defined in baseband (one-sided) as: $B_1 = \frac{1}{T}$ and $B_2 = \frac{0.6}{T}$, where $2T$ is the 4D signal interval. When the pulses $p_1(t)$ and $p_2(t)$ of (2) pass through the channel in (4, 5), they suffer from the combined effects of intersymbol interference (ISI), cross intersymbol interference (CISI) [5], and noise. If $p_{i,k}$ denotes pulse p_i at time $2kT$, i.e., $p_i(t - 2kT)$, ISI is caused by $p_{i,j}$ interfering

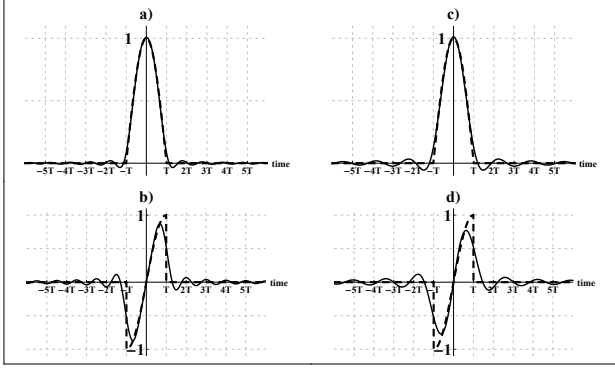


Fig. 1. Filtered (continuous line) and unfiltered (dashed line) cosine and sine pulses. a) p_1 and $p_{1f}(t)$, B_1 . b) p_2 and $p_{2f}(t)$, B_1 . c) p_1 and $p_{1f}(t)$, B_2 . d) p_2 and $p_{2f}(t)$, B_2 (with $B_1 = 1/T$, $B_2 = 0.6/T$).

with $p_{i,k}, j \neq k$ and $i = 1, 2$, and CISI is caused by $p_{1,j}$ interfering with $p_{2,k}$ or $p_{2,j}$ interfering with $p_{1,k}$, for any j, k . The effects of filtering are shown in Fig. 1 for two bandwidths of interest, where the filtered pulses are denoted with the subscript f , and are given by (14) and (15) in the Appendix.

In our performance analysis, we assume that only one past and one future symbol interfere with the current symbol being detected. A total of 83 % of the energy in the half-sine pulse and 99 % of the half-cosine pulse are within a bandwidth of $0.6/T$; of this energy, 99 % and 99.8 %, respectively, is within the interval from $-3T$ and $3T$ (i.e., from $k = -1$ to 1).

IV. COHERENT RECEIVER

At the receiver, the passband received signal is coherently detected in the correlation receiver by multiplying it by the cosine and sine carriers and by the half-cosine and half-sine pulses and then integrating and dumping. In baseband, the receiver ideally separates the real parts from the imaginary parts, and the cosine pulses from the sine pulses by multiplying the filtered signal $s_f(t) = \text{Re}\{s_f(t)\} + j \text{Im}\{s_f(t)\}$ by the original pulses $p_1(t) - jp_2(t)$ if no knowledge of the channel is available, or by the filtered pulses $p_{1f}(t) - jp_{2f}(t)$ if the channel is known. Due to ISI and CISI, the tails of the interfering past and future pulses affect the pulses currently being detected. Considering only the truncated sequence [24] of length equal to three signaling intervals ($k = -1, 0, 1$) and ignoring the noise for now, the signals at the input of the receiver, corresponding to the current signaling interval being detected ($|t| \leq T$) are:

$$s_f(t) = \sum_{k=-1}^1 [b_{1,k}p_{1f}(t-2kT) + b_{2,k}p_{2f}(t-2kT) + j(b_{3,k}p_{1f}(t-2kT) - b_{4,k}p_{2f}(t-2kT))], \quad (6)$$

where p_{1f} and p_{2f} are the filtered pulses shown in Fig. 1 and defined in (14, 15) in the Appendix, and $b_{i,k}$, $i = 1, \dots, 4$ represents bit i at time $(t - 2kT)$; for example, $b_{2,-1}$ is the value of the second component of the 4D vector $[b_1(t+2T) \ b_2(t+2T) \ b_3(t+2T) \ b_4(t+2T)]$, i.e., the

TABLE I
MAGNITUDE OF THE COEFFICIENTS IN (7) FOR TWO CHANNEL BANDWIDTHS FOR Q²PSK AND SAHA'S CEQ²PSK.

$B_1 = \frac{1}{T}$		$B_2 = \frac{0.6}{T}$		N_1	N_2
\hat{c}_1 or \hat{c}_3	\hat{c}_2 or \hat{c}_4	\hat{c}_1 or \hat{c}_3	\hat{c}_2 or \hat{c}_4		
0.989543	0.778107	0.975659	0.687676	128	16
0.992196	0.783469	0.979426	0.699171	256	32
0.994848	0.788830	0.983194	0.710665	128	16
0.994905	0.887331	0.987154	0.820393	256	32
0.997557	0.892692	0.990921	0.831888	512	64
1.000209	0.898053	0.994688	0.843383	256	32
1.000266	0.996554	0.998648	0.953111	128	16
1.002918	1.001915	1.002416	0.964605	256	32
1.005571	1.007276	1.006183	0.976100	128	16

coefficient of the sine pulse p_2 on the cosine carrier, from the previous 4D signaling interval (the immediate past symbol).

We wish to show the output of the correlation receiver. To concisely write the expression for these output values, we use the following notation: Let $P_{i,j}(r, s) = \int_{-T}^T p_i(t-r)p_j(t-s)dt$. We also let $j = 2 - i \bmod 2$, $l = i - (-1)^i$, and $i = 1, \dots, 4$. The coefficients at the output of the receiver, including (finite) ISI and the CISI are given by (7):

$$\hat{c}_i = b_{i,-1}P_{j,j}(0, -2T) + b_{i,0}P_{j,j}(0, 0) + b_{i,1}P_{j,j}(0, 2T) + b_{l,-1}P_{j,3-j}(0, -2T) + b_{l,1}P_{j,3-j}(0, 2T). \quad (7)$$

Given a single past, present, and future symbol, we can easily enumerate the resulting coefficients, which are ± 1 for the unfiltered channel. For the receiver without channel information, these are shown in Table I for the two channel bandwidths we use; the negative value for each is also possible. The numbers listed under the last two columns, N_1 and N_2 , indicate the number of occurrences of each for Q²PSK and Saha's CEQ²PSK, respectively; there are a total of 4096 sequences of length 3 in the former, and 512 in the latter.

V. PERFORMANCE ANALYSIS

We describe performance of the Q²PSK systems based on probability of error versus SNR and spectral efficiency. We discuss each separately.

A. Probability of Bit Error

We quickly derive the probability of error for the Q²PSK systems in this section. We assume AWGN with (one sided) PSD N_0 in each component. If no bandlimiting occurs, such that there is no ISI/CISI, the probability of bit error may be written as [1]:

$$P_{be} = K_d Q \left(\sqrt{\gamma_c \frac{2E_b}{N_0}} \right), \quad (8)$$

where K_d is the error coefficient normalized per two dimensions, and γ_c is the coding gain given by (9):

TABLE II
PARAMETERS OF (8,9) FOR THE Q²PSK SYSTEMS OF INTEREST.

	4D Q ² PSK	4D CEQ ² PSK	unexpanded 16D CEQ ² PSK	expanded 16D CEQ ² PSK
d_0^2	4	8	8	8
d_{min}^2	4	4	4	4
R	1	3/4	3/4	13/16
R_b	1	1	1	1
γ_c	1	3/2	3/2	13/8
K_d	2	3	3	3

$$\gamma_c = \frac{d_o^2}{d_{min}^2} \frac{R}{R_b}, \quad (9)$$

where d_0 and d_{min} are the minimum distances between points in the coded and uncoded constellations, respectively; R_b is the rate in information bits per dimension of the uncoded system and R is the rate of the coded system, again in information bits per dimension [1]. The values of these are shown in Table II for the four systems we discuss here.

A bit error is committed when the interference and noise cause the transmitted bit to cross the zero-threshold. The probability of bit error, P_{be} , for filtered (finite length) Q²PSK and CEQ²PSK is given by (10):

$$\begin{aligned} P_{be} &= \sum_{n=1}^9 P(r < 0 | \hat{c}_i) P(\hat{c}_i) = \sum_{n=1}^9 P(n < -\hat{c}_i) P(\hat{c}_i) \\ &= \sum_{n=1}^9 P(\hat{c}_i) Q\left(\frac{\hat{c}_i}{\sigma}\right) = \sum_{n=1}^9 P(\hat{c}_i) Q\left(\sqrt{\frac{2}{N_0}} \hat{c}_i\right), \end{aligned} \quad (10)$$

where r is the appropriate component of the received signal, the coefficients are those listed in Table I, and $P(\hat{c}_i)$ is $N_1/2048$ for Q²PSK and $N_2/256$ for CE Q²PSK. Notice that the probability of error is higher for the second and fourth components of the 4D vector than for the first and third; this is due to the significantly wider bandwidth of the half-sine pulse, $p_2(t)$, compared to the half-cosine pulse $p_1(t)$. Equations (8, 10) assume the received components are independent; this is never true for the fourth bit of CEQ²PSK, and is not strictly true for any of these systems due to ISI and CISI. Nonetheless, we show in Section VI that (10) is accurate for all SNR of interest.

We define the SNR in dB as $10 \log_{10} \left(\frac{E_b}{2\sigma^2} \right)$, where E_b is the energy per bit and σ^2 is the noise power in each component, so that SNR= E_b/N_0 . We use unity bit energy here.

B. Spectral Performance

Van Wyk presented an expression for the baseband power spectral density (PSD) of coded and uncoded Q²PSK in [25]. If the amplitudes of the waveforms are adjusted to unity, and using the symbol period $T_s = 4T_b = 2T$, Van Wyk's expression for Q²PSK becomes:

$$\frac{S_{Q^2}(f)}{T_s^2} = \frac{4(1 + 64f^2T_b^2)}{\pi^2} \left(\frac{\cos(4\pi fT_b)}{1 - 64f^2T_b^2} \right)^2. \quad (11)$$

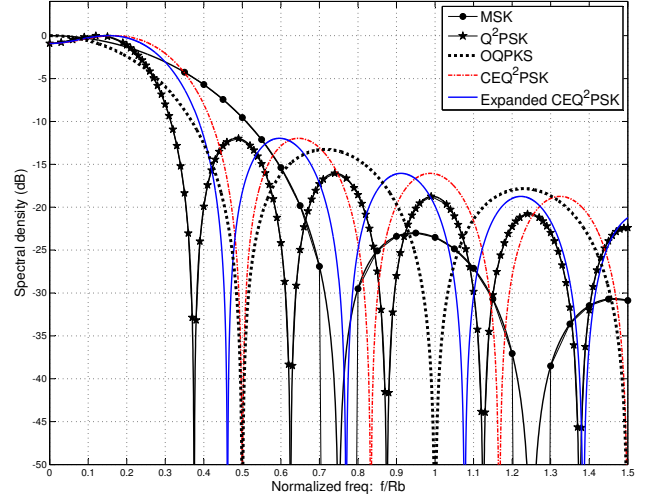


Fig. 2. PSD for systems of interest.

For CEQ²PSK, due to the introduction of the parity check bit, $T_s = 3T_b = 2T$, where the subscript b now indicates information bit; hence,

$$\frac{S_{CEQ^2}(f)}{T_s^2} = \frac{4(1 + 36f^2T_b^2)}{\pi^2} \left(\frac{\cos(3\pi fT_b)}{1 - 36f^2T_b^2} \right)^2, \quad (12)$$

which applies to both Saha's and Cartwright's CEQ²PSK constellations.

Finally, for expanded CEQ²PSK we have a 4D symbol period of $T_s = \frac{13T_b}{4} = 2T$ and (12) becomes

$$\frac{S_{exp}(f)}{T_s^2} = \frac{4 + 169f^2T_b^2}{\pi^2} \left(\frac{\cos(13\pi fT_b/4)}{1 - 169f^2T_b^2/4} \right)^2. \quad (13)$$

Fig. 2 shows the PSD for the systems of interest, in addition to MSK and OQPSK. Non-parametrical spectral estimation was performed using the periodogram method, with 200 spectral averages and using Bartlett windows before performing the FFT. Simulation results confirmed the derivation above (the plots of the simulated values are not shown as they overlap the theoretical lines).

We note that the -3 dB bandwidth of expanded 16D CEQ²PSK is equal to that of MSK, and is 125 % of Q²PSK's. CEQ²PSK has the widest -3 dB bandwidth, and its PSD is similar to that of Offset QPSK [2], in the sense that the first null also occurs at normalized frequency of 0.5. The first null of the expanded constellation is $\frac{6}{13T_b} = \frac{0.4615}{T_b}$, 61 % of that of MSK, while it is 67 % for CEQ²PSK and 50 % for Q²PSK.

Q²PSK has the narrowest main lobe, but the first side lobe has the same peak energy as those of both CEQ²PSK systems. MSK's main lobe is the widest, with considerably lower and wider sidelobes. The sidelobe peaks decrease most slowly for CEQ²PSK (expanded and unexpanded).

VI. RESULTS

We present simulation results for 4D Q²PSK, Saha's 4D CEQ²PSK, and 16D TCM CEQ²PSK for ideal bandlimited

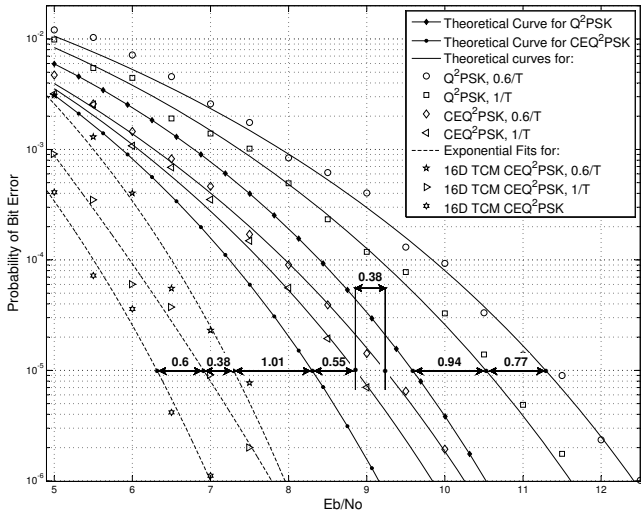


Fig. 3. BER for Q^2PSK , CEQ^2PSK and 16D TCM CEQ^2PSK systems, filtered and unfiltered, when receiver has no knowledge of the channel.

channels of baseband bandwidth $1/T$ and $0.6/T$, along with theoretical performance curves, when available. Unfilled markers show simulation results obtained counting at least 20 bit errors.

Fig. 3 shows a comparison of the bit error rates (BER) for filtered and unfiltered Q^2PSK , 4D CEQ^2PSK , and 16D TCM CEQ^2PSK at the two bandwidths of interest using no channel estimation. We see in Fig. 3 that the TCM system provides about 2 dB of gain over the equivalent uncoded system for all channel bandwidths, requiring only 7.3 dB in SNR for a probability of bit error of 10^{-5} when bandlimited to $0.6/T$ baseband bandwidth. We also confirm that Q^2PSK requires about 11.2 dB of SNR for a bit error rate (BER) of 10^{-5} , as stated by Saha in [3], for a filter of bandwidth $0.6/T$; we note, however, that Saha used a sixth-order Butterworth filter. Losses due to finite channel bandwidth are most severe for Q^2PSK .

Figs. 4 and 5 allow us to compare the receivers with channel knowledge (receiver 2) to those that do not assume any knowledge of the channel (receiver 1). Fig. 4 shows our results for a channel bandlimited to $0.6/T$ while Fig. 5 shows the same curves for a channel of bandwidth $1/T$. The gains achieved by using channel estimation are clearly shown on the plots.

Saha stated in [2] that MSK needs 9.6 dB of SNR to achieve $P_{be} = 10^{-5}$ when filtered at $0.6/T$ and, in [3], that CEQ^2PSK requires 10.3 dB using a sub-optimum bit-by-bit detector. We have shown in Fig. 4 that CEQ^2PSK achieves $P_{be} = 10^{-5}$ at an SNR of 9.3 dB if a sequence detector with no channel information is used instead, and only 8.8 dB if channel estimation is performed so that the filtered pulses are used in the receiver. Cartwright and Kaminsky [11] showed that an SNR of 8.3 dB is actually needed if the channel is not bandlimited, which is confirmed in Fig. 3.

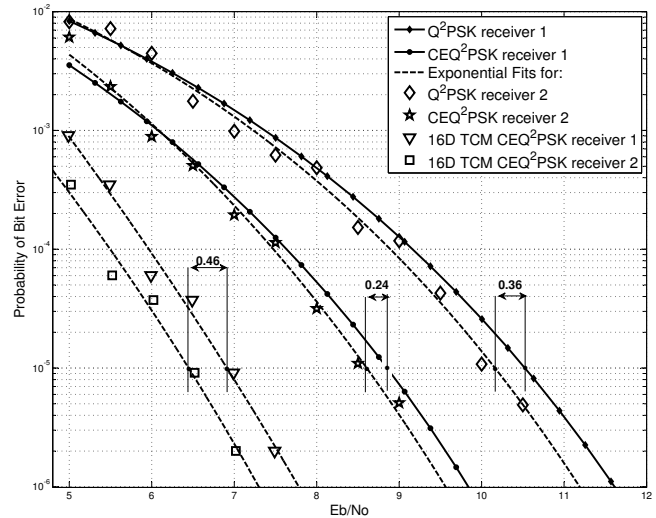


Fig. 4. BER for Q^2PSK , CEQ^2PSK and 16D TCM CEQ^2PSK systems filtered at $0.6/T$ with receivers with and without channel knowledge (labeled receiver 2 and 1, respectively).

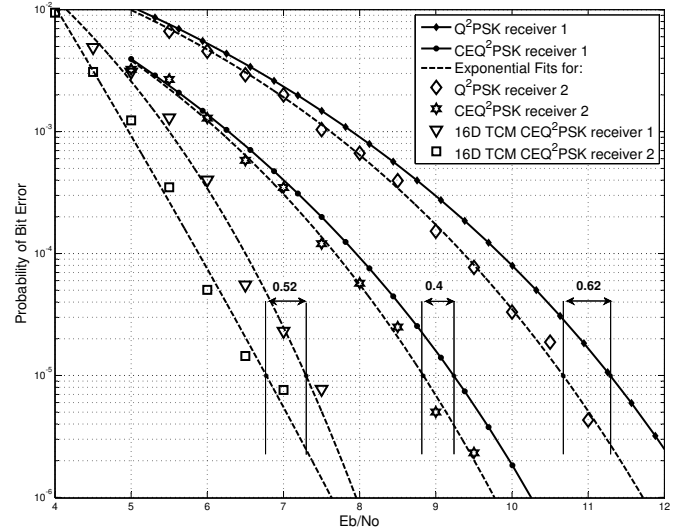


Fig. 5. BER for Q^2PSK , CEQ^2PSK and 16D TCM systems filtered at $1/T$ with receivers with and without channel knowledge (labeled receiver 2 and 1, respectively).

For channel bandwidth of $0.6/T$, when TCM is used with the expanded 16D constellation, we achieve a BER of 10^{-5} with 7.3 dB if no knowledge of the channel is assumed (receiver 1) and with only 6.8 dB if knowledge of the channel (receiver 2) is assumed; the penalty paid for this gain is increased complexity in the receiver. The same conclusions are drawn about gains for channels with a bandwidth of $1/T$, as shown on Fig. 5. Notice, however, that at $1/T$ Q^2PSK gains less than the TCM system, while at $0.6/T$ the gain is larger. The gain due to knowledge of the channel is always smallest for 4D CEQ^2PSK .

Using channel estimation aids the 16D TCM system more than the 4D uncoded equivalent and knowledge of the channel

is more important for Q²PSK than for its constant envelope counterpart.

VII. CONCLUSIONS

We have presented the performance of Q²PSK and its variants CEQ²PSK and 16D TCM CEQ²PSK in ideal bandlimited channels with and without channel knowledge at the receiver. We have noted that the effect of bandlimitation to $0.6/T$, with T the 2D signaling interval, results in a needed increase of between between 1 dB and 1.7 dB in SNR for a BER of 10^{-5} if no channel estimation is used and around 0.5 dB if knowledge of the channel is assumed. The best performance among the systems studied is that of the 16 TCM CEQ²PSK system which requires less than 6.8 dB of SNR for that BER in the most severe bandlimitation, but requires a more complex receiver.

Future work will include simulations of the constant envelope 4D and 16D systems in fading channels and in the nonlinear satellite channel, where use of constant envelope systems becomes most important. Use of pulses that have narrower bandwidth such as those in [5] should also be evaluated in bandlimited channels. Phase estimation algorithms along with actual causal bandlimited channel models should be incorporated. We will also perform the analysis of ISI/CISI for Cartwright's CEQ²PSK constellation, which is expected to be less affected by interference than Saha's.

REFERENCES

- [1] G. Forney and G. Ungerboeck, "Modulation and coding for linear Gaussian channels," *IEEE Trans. Inf. Theory*, vol. 44, no. 6, pp. 2384–2415, 1998.
- [2] D. Saha and T. G. Birdsall, "Quadrature-quadrature phase shift keying," *IEEE Trans. Commun.*, vol. 37, no. 4, pp. 437–448, March 8, 1989.
- [3] D. Saha, "Quadrature-quadrature phase shift keying with constant envelope," US Patent 4,730,344, March, 1988.
- [4] B. H. Waldeck, S. A. Swanepoel, and L. P. Linde, "TFO Q²PSK: A multi-dimensional spectrally efficient modulation scheme," in *Proc. 1998 South African Symp. Commun. Signal Proc.*, Sep 1998, pp. 39–42.
- [5] M. Fertat, W. Zschunke, and A. Bertraissoul, "Spectral optimization of QPSK and Q²PSK systems using timelimited and zero-ISI pulse shaping," *Frequenz*, vol. 57, no. 9–10, pp. 197–203, 2003.
- [6] M. Visintin, E. Biglieri, and V. Castellani, "Four-dimensional signaling for bandlimited channels," *IEEE Trans. Commun.*, vol. 42, no. 234, pp. 403–409, 1994.
- [7] B. Westra, D. Van Wyk, J. Cilliers, and L. Linde, "Performance evaluation of multi-level four-dimensional Q²PSK in Gaussian noise," in *Proc. COMSIG 97, South African Symp. Commun. Signal Proc.*, Sept. 1997, pp. 141–146.
- [8] D. Saha and O. El-Ghandour, "Differentially coherent quadrature-quadrature phase shift keying (Q²PSK)," in *Conf. Record IEEE MIL-COM '90, Military Commun. Conf.*, vol. 2, Sep 1990, pp. 585–589.
- [9] V. Acha and R. Carrasco, "A new digital implementation of quadrature-quadrature phase shift keying," in *Proc. Third IEE Conference on Telecommunic.*, Mar 1991, pp. 29–34.
- [10] I. Korn and L. Wei, "Q²DPSK in the satellite mobile channel with ISI and CSI," *IEEE Trans. Veh. Technol.*, vol. 43, no. 1, pp. 69–78, Feb. 1994.
- [11] K. V. Cartwright and E. J. Kaminsky, "An optimum hardware detector for constant envelope quadrature-quadrature phase-shift keying (CEQ²PSK)," in *Proc. IEEE GLOBECOM'05*. St. Louis, MO: IEEE, 28 Nov.–2 Dec. 2005, pp. 393–396.
- [12] J. Cilliers and L. P. Linde, "Performance of an adaptive multi-dimensional lattice equaliser for Q²PSK over multipath channels," in *Proc. IEEE AFRICON 2001, 6th. Africon Conf. in Africa*, vol. 1, Oct 2002, pp. 155–160.

- [13] M. Quinteros, E. J. Kaminsky, and K. Cartwright, "A trellis-coded modulation scheme with a novel expanded 16-dimensional constant envelope Q²PSK constellation," in *Proc. IEEE GLOBECOM 2009*, Honolulu, HI, USA, Dec. 2009, pp. 1–6.
- [14] V. Acha and R. Carrasco, "Trellis coded Q²PSK signals. I. AWGN and nonlinear satellite channels," *IEE Proc. -Commun.*, vol. 141, no. 3, pp. 151–158, June 1994.
- [15] J. S. Han and M. J. Kim, "Offset quadrature-quadrature phase shift keying with half-sine pulse shaping," in *Proc. ICTC 2013, Internat. Conf. Convergence*, 2013, pp. 931–935.
- [16] K. Priya and M. Tamilarasi, "A trellis-coded modulation scheme with 32-dimensional constant envelope Q²PSK constellation," in *Proc. ICCSP 2013 conf., Commun. Signal Proc.*, 2013, pp. 821–825.
- [17] M. I. Quinteros, E. J. Kaminsky, K. V. Cartwright, and R. U. Gallegos, "A novel expanded 16-dimensional constant envelope Q²PSK constellation," in *Proc. IEEE TechCon 2008, Region 5 Conference*. Kansas City, MO: IEEE, April 17–20 2008, pp. 1–6.
- [18] L.-F. Wei, "Trellis-coded modulation with multidimensional constellations," *IEEE Trans. Inf. Theory*, vol. IT-33, no. 4, pp. 483–501, July 1987.
- [19] D. Saha, "Channel coding with quadrature-quadrature phase shift-keying (Q²PSK) signals," *IEEE Trans. Commun.*, vol. 38, pp. 409–417, Apr. 1990.
- [20] D. Van Wyk and L. Linde, "Hybrid block-convolutional rate-1/2 coding strategy for constant envelope CEQ²PSK," *Electronics Letters*, vol. 32, no. 24, pp. 2204–2206, 1996.
- [21] E. J. Kaminsky, "Trellis coding and adaptive estimation in dually polarized systems," Ph.D. Dissertation, Tulane University, Department of Electrical Engineering, New Orleans, LA 70118, June 1991.
- [22] E. Kaminsky, J. Ayo, and K. Cartwright, "TCM without constellation expansion penalty," *IKCS-IEEE J. Commun. and Networks*, vol. 4, no. 2, pp. 90–96, June 2002.
- [23] J. M. Wozencraft and I. M. Jacobs, *Principles of communication engineering*. John Wiley & Sons, 1965.
- [24] O. Shimbo and M. Celebiler, "The probability of error due to intersymbol interference and Gaussian noise in digital communication systems," *IEEE Trans. Commun. Technol.*, vol. 19, no. 2, pp. 113–119, 1971.
- [25] D. Van Wyk, "Four-dimensional Q²PSK modulation and coding for mobile digital communication," Master's Thesis, University of Pretoria, South Africa, April 1996.

APPENDIX

The expressions for the filtered half-cosine and half-sine pulses, p_{1f} and p_{2f} are presented here. Convolution of the channel impulse response $h(t)$ with the Q²PSK pulses yields:

$$\begin{aligned}
 p_{1f}(t) = & \frac{1}{2\pi} \sin(\omega_\alpha t) [\text{Ci}((t-T)(\omega_\alpha + \omega_\beta)) + \\
 & - \text{Ci}((t+T)(\omega_\alpha + \omega_\beta)) + \text{Ci}((t+T)(\omega_\beta - \omega_\alpha)) + \\
 & - \text{Ci}((t-T)(\omega_\beta - \omega_\alpha))] + \\
 & + \frac{1}{2\pi} \cos(\omega_\alpha t) [\text{Si}((t+T)(\omega_\beta - \omega_\alpha)) + \\
 & - \text{Si}((t-T)(\omega_\beta - \omega_\alpha)) + \text{Si}((t+T)(\omega_\alpha + \omega_\beta)) + \\
 & - \text{Si}((t-T)(\omega_\alpha + \omega_\beta))] .
 \end{aligned} \tag{14}$$

$$\begin{aligned}
 p_{2f}(t) = & \frac{1}{2\pi} \sin(\omega_\alpha t) [\text{Si}((t+T)(\omega_\alpha + \omega_\beta)) + \\
 & - \text{Si}((t-T)(\omega_\alpha + \omega_\beta)) + \text{Si}((t+T)(\omega_\beta - \omega_\alpha)) + \\
 & - \text{Si}((t-T)(\omega_\beta - \omega_\alpha))] + \\
 & + \frac{1}{2\pi} \cos(\omega_\alpha t) [\text{Ci}((t+T)(\omega_\alpha + \omega_\beta)) + \\
 & - \text{Ci}((t-T)(\omega_\alpha + \omega_\beta)) - \text{Ci}((t+T)(\omega_\beta - \omega_\alpha)) + \\
 & + \text{Ci}((t-T)(\omega_\beta - \omega_\alpha))] .
 \end{aligned} \tag{15}$$

where $\omega_\alpha = \frac{\pi}{2T}$ and $\omega_\beta = 2\pi B$, and the cosine and sine integrals, Ci and Si, are defined in (16):

$$\text{Ci}(x) = - \int_x^\infty \frac{\cos t}{t} dt, \quad \text{Si}(x) = \int_0^x \frac{\sin t}{t} dt. \tag{16}$$